

## Electron Heating Mechanisms in Helium rf Glow Discharges: A Self-Consistent Kinetic Calculation

T. J. Sommerer,<sup>(a)</sup> W. N. G. Hitchon,<sup>(b)</sup> and J. E. Lawler<sup>(a)</sup>

*University of Wisconsin, Madison, Wisconsin 53706*

(Received 22 August 1989)

Power dissipation mechanisms in low-pressure helium radio-frequency glow discharges are studied using a model which is able to describe the discharge at the kinetic level with a self-consistent electric field. We find a low average electron energy ( $< 1$  eV) in the bulk plasma and a weak electric field ( $\approx 2$  V/cm) that is largely out of phase with the sheath fields. The weak bulk field is shown to be important for heating electrons of all energies.

PACS numbers: 51.10.+y, 52.20.-j, 52.80.Hc

Fully self-consistent kinetic models of radio-frequency (rf) discharge plasmas are now possible using the "convective scheme" (CS).<sup>1-4</sup> Much progress toward understanding rf discharges has been made with more traditional models using the local-field approximation,<sup>5</sup> Monte Carlo simulations,<sup>6,7</sup> fluid approximations,<sup>8</sup> and other related approaches. Major challenges, such as the energy balance of the bulk electrons, are not easily addressed once the approximations inherent in these models have been made. Traditional models have sidestepped the energy balance of the bulk electrons by predicting only a density-temperature product,<sup>9</sup> calculating a spatially averaged energy balance for a restricted range of parameters,<sup>10</sup> or simply assuming a 1-eV average bulk electron energy.<sup>11</sup> A recent experiment shows that the average energy of the bulk electrons can be astonishingly low (0.043 eV).<sup>12</sup> We report in this Letter a fully kinetic model for rf discharge plasmas with a self-consistent electric field, and we use this model to study the energy balance of the bulk electrons.

An efficient numerical scheme based on propagators (Green's functions)<sup>1-4</sup> is employed here to yield distribution functions consistent with Poisson's equation for the electrons and ions in four He rf discharges. The kinetic model of the electrons described in Ref. 4 is modified<sup>13</sup> and combined with Poisson's equation and a kinetic description of the ions to yield a fully self-consistent, kinetic model. Energy loss by electrons during elastic col-

lisions with neutrals has also been added here.

Calculations are typically started with a spatially uniform density of ions and electrons and run in the applied rf potential until the fractional change over a cycle in key quantities is less than a chosen value  $c$ . Typically,  $c < 5 \times 10^{-4}$ . Running to harmonic convergence is a most difficult problem because number densities (for instance) may continue to change by small amounts for many rf cycles. To avoid excessive computation times a run may be stopped, the particle densities adjusted (while preserving the net charge density at all spatial locations and hence the instantaneous field configuration), and then resumed from that point. The true final densities can thus be bracketed. We estimate that the present results differ from those of a perfectly converged solution by  $< 15\%$  in absolute densities, better in most other variables.

Four sets of discharge conditions were considered. Most discussion will center on a "benchmark" 0.1-Torr He discharge with a gap of  $d = 4$  cm, operating at a frequency  $f_0 = 13.56$  MHz with an applied sinusoidal voltage  $V^0 = 500$  V (peak). We assume 0.1 electron on average is released from an electrode per incident ion ( $\gamma = 0.1$ ). Each of the other three discharges differs in one parameter:  $V^0$ ,  $f_0$ , or  $\gamma$ . The results are summarized in Table I.

Results from the converged benchmark solution are shown in Fig. 1 over one rf cycle. The sheath electric

TABLE I. Summary of the results from the four He rf discharges. All discharges have an electrode spacing  $d$  of 4 cm and a neutral He density  $N$  of  $3.535 \times 10^{15}$  cm<sup>-3</sup>. The plasma potential, bulk ionization rate, and bulk average energy have been averaged over one rf cycle. The benchmark run is labeled "1."

Run number	Potential amplitude $V^0$ (V)	rf frequency $f_0$ (MHz)	Secondary coefficient $\gamma$	Current density $j_b^0$ (mA cm <sup>-2</sup> )	Plasma potential $V^{dc}(d/2)$ (V)	Maximum sheath length $L^{\max}$ (cm)	Peak plasma density $n^{\max}$ ( $10^9$ cm <sup>-3</sup> )	Peak ionization rate $S^{\max}$ ( $10^{14}$ cm <sup>-3</sup> s <sup>-1</sup> )	Bulk ionization rate $S(d/2)$ ( $10^{14}$ cm <sup>-3</sup> s <sup>-1</sup> )	Bulk average energy $\langle \tau(d/2) \rangle$ (eV)	Bulk electric field $E^0(d/2)$ (V/cm)
1	500	13.56	0.1	2.7	221	1.1	10.2	9.0	5.5	0.54	1.9
2	500	10	0.1	1.5	219	1.4	3.6	5.3	3.2	0.90	1.9
3	500	13.56	0.0	2.6	222	1.1	9.0	8.3	5.0	0.58	1.8
4	250	13.56	0.1	1.3	121	1.1	3.6	2.8	1.7	0.68	1.8

fields [Fig. 1(a)] are dominantly linear, reflecting a nearly constant (space and time) ion density outside the bulk and the dynamic action of the more mobile electrons as they move to neutralize ions in this region when the instantaneous field is small. (“Bulk” here refers to locations where the time-averaged field is weak; “sheath” refers to locations where the instantaneous field is strong.) The ion plasma frequency is of the order of the

rf frequency; the ion density is nearly constant over a cycle, while the ion current to each electrode varies by around 30%. The electric field in the bulk ( $E_{\text{bulk}}$ ) oscillates with a (roughly) spatially uniform amplitude of 1.9 V/cm. Surprisingly,  $E_{\text{bulk}}$  is largely out of phase with the sheath fields, and is distinctly nonsinusoidal (Fig. 2). The field reversal occurs at the base of a given sheath while the sheath is reaching its maximum extent and also during the subsequent contraction. Conversely, the reversal is at the opposite side of the bulk when a sheath is minimal in extent and during the next expansion. The time-averaged fields in the bulk are roughly consistent with an ambipolar diffusion loss of ions.<sup>14</sup>

The average energy of the bulk electrons is low, averaging 0.54 eV over an rf cycle at the center of the discharge. Experiments have seen similar or even lower bulk electron temperatures in various He rf (Ref. 12) and dc (Ref. 14) discharges. At this pressure (0.1 Torr), the mean free path for ionization in He is several discharge lengths, and the ionization is due to high-energy electrons streaming through the discharge, as in a negative glow region or a beam-sustained discharge. The ionization rate (per unit volume) therefore peaks near the sheath-bulk boundary [Fig. 1(b)] as electrons that had migrated toward the electrode during the anodic part of the cycle are accelerated by the expanding sheath [Fig. 1(a)] during the cathodic phase. These discharges all appear to operate in a regime where sheath expansion is the dominant electron heating mechanism.<sup>7,9,11</sup> Figure 1(c) shows the deposition of power into the electrons; energy is given to the electrons during sheath expansion, but also flows from the particles into the field during sheath contraction. Bulk ion loss is dominated by a process analogous to ambipolar diffusion; that is, the product of the ion density, ion mobility, and average energy of the bulk electrons is approximately

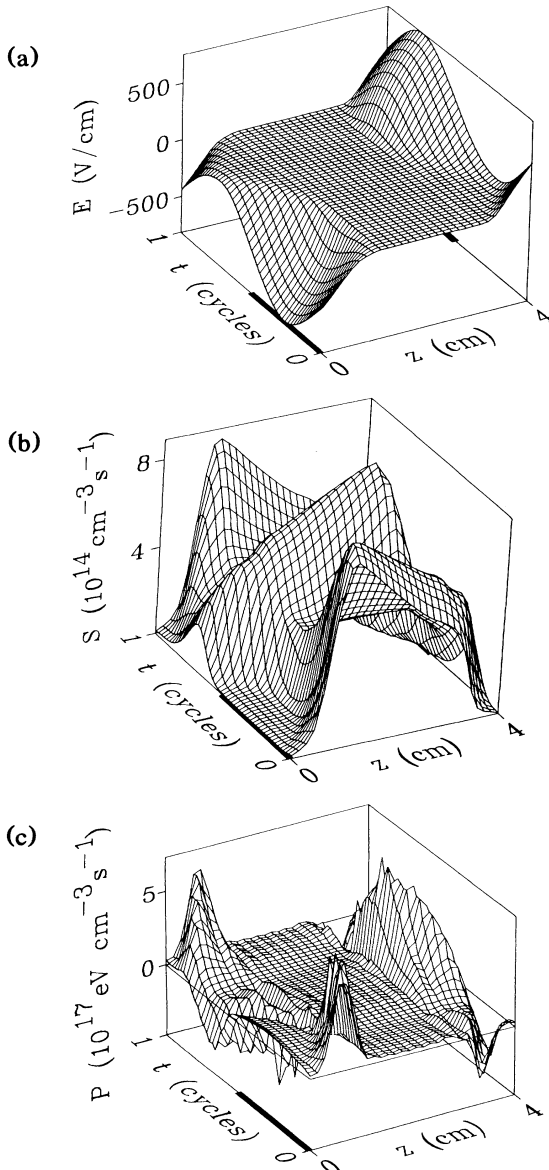


FIG. 1. Benchmark run: (a) electric field  $E(z,t)$ , (b) primary ionization rate per unit volume  $S(z,t)$ , and (c) power deposition into the electrons  $P(z,t) = -n_e |e| E_z \langle v_z \rangle$ , over one rf cycle  $T = 7.375 \times 10^{-8}$  s. The heavy portions of the  $z = 0$  and  $z = 4$  cm lines indicate parts of the rf cycle where the corresponding electrode is cathodic.

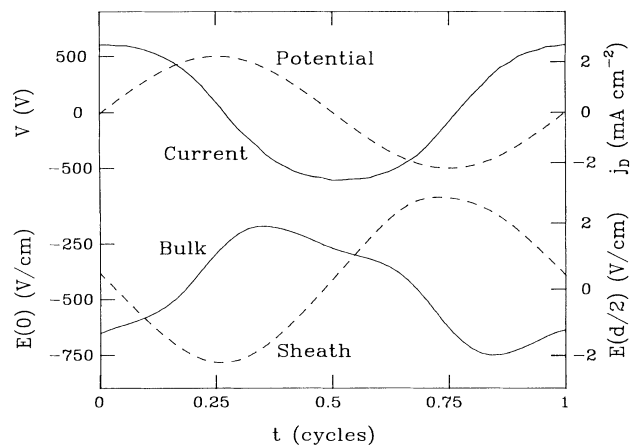


FIG. 2. The applied potential, discharge current, electric field at the  $z = 0$  electrode, and bulk electric field ( $z = d/2$ ) of the benchmark discharge over one rf cycle  $T$ .

equal to the product of the diffusion length squared and the average ionization rate.<sup>14</sup>

"Tracking" calculations utilizing the results of this benchmark discharge were used to examine the behavior of the bulk electrons. These runs were started when the left electrode was most cathodic [ $t=T/4$  in Fig. 1(a)]. The electron distribution was cleared except for bulk electrons at one selected speed. These electrons were then followed for one or more cycles using the electric field and other results from the benchmark run as input to the tracking calculation. The true benchmark field was used initially. The role of  $E_{\text{bulk}}$  in heating these electrons was clarified by modifying the benchmark field and performing identical tracking runs. Two variations were used: The first was to simply set  $E_{\text{bulk}}$  to zero, and the second was to invert the sign of  $E_{\text{bulk}}$ . The strong sheath fields were not modified.

Low-energy (0.5-eV) bulk electrons respond to the bulk field, but require on the order of an rf cycle ( $T=7.375 \times 10^{-8}$  s) to cross the bulk and undergo several collisions during the crossing. The sheaths move with speeds of up to  $\approx 5 \times 10^7$  cm/s [see Fig. 1(a)]. Low-energy electrons are gently pushed by  $E_{\text{bulk}}$  toward an electrode as the sheath retreats toward that electrode during the anodic part of the cycle. They move too slowly to catch the retreating sheath, bounce, and lose energy. These slow electrons are unable to move away during the subsequent sheath expansion, and are heated as the sheath moves past. Setting  $E_{\text{bulk}}$  to zero or inverting it inhibits the coldest electrons from moving in behind the retreating sheath and halves the total ionization due to these low-energy electrons during the first tracking cycle.

Higher-energy (15-eV) electrons can cross the bulk several times per rf cycle and have twice the mean free path of the 0.5-eV electrons; they can cross the bulk and collide with a sheath at any time. They gain energy from the field during collisions with expanding sheaths and lose energy to the field upon hitting a contracting sheath [Fig. 1(c)], and the energy gain or loss is dependent upon the relative speed of the electron and sheath.  $E_{\text{bulk}}$  hinders heating of these high-energy electrons because for most of an rf cycle it slows electrons moving toward expanding sheaths and accelerates them toward contracting sheaths. Inverting or zeroing  $E_{\text{bulk}}$  aids electron heating by the expanding sheaths and increases total ionization during the first tracking cycle by  $\approx 20\%$ .

An overwhelming majority of the discharge electrons have energies less than 1 eV, and only a tiny fraction of these cold electrons need be heated and subsequently ionize neutral atoms to sustain the discharge. Obtaining the correct  $E_{\text{bulk}}$  and a realistic picture of the power balance is a prerequisite for a quantitative understanding of plasma chemistry. The 0.043-eV electrons observed by Hebner, Verdeyen, and Kushner<sup>12</sup> in He could attach to an electronegative gas and form negative ions, while the several-eV electrons predicted by Kushner<sup>7,15</sup> (various

molecular gases) and Graves and Jensen<sup>8</sup> (fictitious gas) would dissociate many molecular species. Though the Ar-SiH<sub>4</sub> discharges studied by Kushner<sup>7</sup> differ greatly from these He discharges, his conclusions regarding the magnitude of  $E_{\text{bulk}}$  needed for significant bulk heating are largely applicable here. Power is not directly deposited into the bulk electrons in great quantity [Fig. 1(c)] in these discharges, but  $E_{\text{bulk}}$  is the only source of energy for the coldest electrons. In one rf cycle even the coldest bulk electrons can gather sufficient energy from  $E_{\text{bulk}}$  to be efficiently heated by the expanding sheaths.

The huge amount of information available in these kinetic calculations is evident in Fig. 3, which shows the isotropic part of the electron velocity distribution function (EVDF) of the benchmark run when the left electrode is most cathodic. There are very few electrons in the sheath. The secondary electrons liberated from the left electrode and accelerated to the sheath potential are clearly shown, as is the very low average energy of the bulk electrons. The full angular distributions corresponding to Fig. 3 shows the expected beam of secondaries traveling in the  $+z$  direction and an isotropic distribution of low-energy electrons. The electrons in the local maximum in  $f$  at  $\tau \approx 250$  eV are secondaries which have been scattered and are moving transverse to the discharge axis.

Table I summarizes the three other calculations. The  $E_{\text{bulk}}$  wave forms were remarkably similar for all of these discharges. The current leads the applied voltage by almost  $\pi/2$ , and is nearly sinusoidal (only the  $3f_0$  harmonic, at 5%–7%, was more than 1% of the fundamental  $f_0$ ).

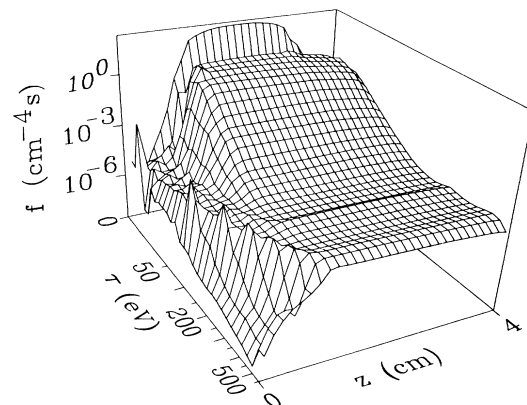


FIG. 3. Isotropic part of the EVDF of benchmark run. The left electrode is most cathodic at this phase of the rf cycle.  $f = \sum_{\mu} N^{z\mu} / A \Delta z \Delta v$ , where  $N^{z\mu}$  is the number of electrons in one mesh cell centered at  $z$ ,  $v$ , and  $\mu = \cos\theta$ .  $\Delta z$ ,  $\Delta v$ , and  $\Delta \mu$  are the dimensions of the cell, and  $A$  is the area of the discharge. The energy axis is equally spaced in velocity, but labeled in energy units for convenience ( $\tau = mv^2/2$ ). Note the overwhelming number of low-energy electrons and the beam of electrons ejected from the  $z=0$  electrode. The spikes in this beam are an artifact of the energy-conserving algorithm and the finite mesh size.

The ionization rates were all of the same form as Fig. 1(b), though differing significantly in magnitude. The similarity of the ionization rates of runs 1 and 3, which differ only in  $\gamma$ , shows that the electrons ejected from the electrodes by ion impact play only a minor role in these discharges. Run 2 differed from the benchmark by only 26% in rf frequency, yet differed markedly in overall ionization rate, plasma density, and bulk average energy.

We have used a self-consistent kinetic calculation of rf discharges to study the energy balance of the bulk electrons. The dominant electron heating mechanism in the discharges studied here is sheath expansion, yet the bulk electric field feeds energy into the coldest bulk electrons (which are the most numerous) and improves the efficiency of the sheath-expansion heating mechanism. It reduces the energy gained by higher-energy electrons by accelerating them toward contracting sheaths, where they bounce and lose energy, and slowing their movement toward expanding sheaths, where they gain energy. These kinetic calculations, in addition to addressing difficult challenges such as the energy balance of the bulk electrons, will enable us to explore the limits of various traditional approximations. They make possible accurate *a priori* predictions of discharge properties that are limited only by the quality of the physical approximations and the accuracy of the available electron emission coefficient and cross-section data.

This work was supported by the Air Force Office of Scientific Research.

<sup>(a)</sup>Department of Physics.

<sup>(b)</sup>Department of Electrical and Computer Engineering.

<sup>1</sup>J. B. Adams and W. N. G. Hitchon, *J. Comput. Phys.* **76**, 159 (1988).

<sup>2</sup>W. N. G. Hitchon, D. J. Koch, and J. B. Adams, *J. Comput. Phys.* **83**, 79 (1989).

<sup>3</sup>W. N. G. Hitchon, *J. Plasma Phys.* **41**, 323 (1989).

<sup>4</sup>T. J. Sommerer, W. N. G. Hitchon, and J. E. Lawler, *Phys. Rev. A* **39**, 6356 (1989).

<sup>5</sup>J. P. Boeuf, *Phys. Rev. A* **36**, 2782 (1987).

<sup>6</sup>R. W. Boswell and I. J. Morey, *Appl. Phys. Lett.* **52**, 21 (1988).

<sup>7</sup>Mark J. Kushner, *IEEE Trans. Plasma Sci.* **14**, 188 (1986).

<sup>8</sup>David B. Graves and Klavs F. Jensen, *IEEE Trans. Plasma Sci.* **14**, 78 (1986).

<sup>9</sup>V. A. Godyak and A. S. Khanneh, *IEEE Trans. Plasma Sci.* **14**, 112 (1986).

<sup>10</sup>G. R. Misium, A. J. Lichtenberg, and M. A. Lieberman, *J. Vac. Sci. Technol. A* **7**, 1007 (1989).

<sup>11</sup>J. P. Boeuf and Ph. Belenguer, in "Non-equilibrium Processes in Partially Ionized Gases," Proceedings of the NATO Advanced Study Institute, Acquafredda di Maretea, Italy, 4-17 June 1989 (to be published).

<sup>12</sup>G. A. Hebner, J. T. Verdeyen, and M. J. Kushner, *J. Appl. Phys.* **63**, 2226 (1988).

<sup>13</sup>W. N. G. Hitchon, T. J. Sommerer, and J. E. Lawler, in Proceedings of the Seventh IEEE Pulsed Power Conference, Monterey, California, 11-14 June 1989 (to be published).

<sup>14</sup>E. A. Den Hartog, T. R. O'Brian, and J. E. Lawler, *Phys. Rev. Lett.* **62**, 1500 (1989).

<sup>15</sup>M. J. Kushner, *J. Appl. Phys.* **54**, 4958 (1983).